

APPLICATION OF DYNAMICAL SYSTEMS THEORY TO TRAJECTORY DESIGN FOR A LIBRATION POINT MISSION

B. T. Barden* and K. C. Howell†
Purdue University, West Lafayette, Indiana 47907

M. W. Lo‡
Jet Propulsion Laboratory, Pasadena, California 91109

Abstract

Recently, there has been accelerated interest in missions utilizing trajectories near libration points. The trajectory design issues involved in missions of such complexity go beyond the lack of preliminary baseline trajectories (since conic analysis fails in this region of the solution space). Successful and efficient design of mission options will require new perspectives and a more complete understanding of the solution space is imperative. In this investigation, dynamical systems theory is applied to better understand the geometry of the phase space in the three-body problem via stable and unstable manifolds. Then, the manifolds are used to generate various solution arcs and establish trajectory options that are then utilized in preliminary design for the proposed Sues-Urey mission.

Introduction

In astrodynamics, the complex missions envisioned for the upcoming decades will demand innovative spacecraft trajectory concepts. It is also increasingly apparent that accomplishment of many short- and long-term science and exploration goals will require a broader view that expands the range of options available. Most recently, for example, the space science community has had a high level of interest in missions to the vicinity of the libration points in the Sun-Earth system. Spacecraft in orbits near libration points offer valuable opportunities for investigations concerning solar and heliospheric effects on planetary environments. Current design capabilities for such missions have significantly improved in the last five years but are still limited. Computational approaches to determine a nominal trajectory are essentially manual numerical searches in a regime where conic approximations are not adequate; standard targeting and optimization strategies based on linear varia-

tional methods are difficult to apply and frequently break down because of the nonlinearities and high sensitivities in the problem. At the same time, recent evidence supports the theory that the rich dynamics in this region of space may lead to previously undiscovered types of trajectory solutions. Conventional tools simply do not incorporate any firm theoretical understanding of the multi-body problem and do not offer the flexibility to take further advantage of the dynamical relationships in producing alternative trajectory designs. Nonlinear dynamical systems theory may offer much insight, particularly in multi-body regimes, where qualitative information is needed concerning sets of solutions and their evolution. For example, invariant manifolds associated with a family of periodic orbits have already served as a guide to generate natural pathways near the libration points¹⁻⁵. But the primary objective here is to *use* this information for trajectory design.

Trajectory design has traditionally been initiated with a baseline mission concept rooted in the two-body problem and conics. Design algorithms built on conics use trajectory arcs from a limited set of possible types, i.e., ellipses, parabolas, and hyperbolas. For libration point missions, however, a baseline concept derived from solutions to the three-body problem is required. Since no such general solution is available, the primary goal is to use dynamical sys-

*Graduate Student, School of Aeronautics and Astronautics, Member AIAA

†Associate Professor, School of Aeronautics and Astronautics, Senior Member AIAA, Member AAS

‡Member of Technical Staff

tems theory to systematically numerically explore the types of solution arcs that may be available (as well as general behavior in various regions of the phase space) for design in the three-body problem. The secondary goal is to use the information to guide the mission design process for the proposed Suess-Urey mission by patching various segments together. Preliminary design is accomplished in the context of the restricted problem of three bodies, and then the solution is computed using a model that incorporates ephemeris data as well as solar radiation pressure.

Background

Much success has been achieved in mission design and analysis with traditional approaches (including conic analysis). Standard analytical and numerical methods do provide very accurate information, even for multi-body problems, because the present techniques can very accurately represent the evolution of a particular trajectory. The most challenging interplanetary missions involving multiple gravity assists have been designed with such tools. However, only a limited region of the orbit design space has actually been exploited thus far. In this view, it is then necessary to generalize the baseline model and explore larger regions of the solution space in the general n -body problem. An extension to increase the complexity of the model in the basic problem is the examination of three- and four-body systems. After 200 years, the three-body problem remains unsolved, but, in the last 20 years, substantial progress has been made in recognizing that the unique dynamic characteristics in the problem can be used for mission design. The trigger that refocused interest in the problem was the discovery of new types of particular solutions in the three-body problem: periodic halo orbits and quasi-periodic Lissajous trajectories. These trajectories (three-dimensional in configuration space) are not found in the region of the solution space occupied by solutions to the two-body problem. A number of missions have already incorporated Lissajous and/or halo orbits as part of the trajectory design: ISEE-3 (1978 launch), WIND (currently en route to arrive in 1997), SOHO (1995 launch), ACE (1997 launch), and others currently in development. It is not a coincidence that the trajectories employed in these missions are all somewhat similar. Without a firm theoretical understanding of this region of the solution space, trajectory design for these types of missions typically relies on past numerical search results for guidance in the construction of baseline trajectories. While this approach has clearly resulted in very successful flight paths, increased science opportunities will demand more flexibility and a

better understanding of the design process. To make real progress on these mission design issues, it is important to view this as a problem in *mechanics*, not numerical analysis. Of course, without a general solution to this nonlinear problem, numerical analysis is still critically necessary. But clever, less costly solutions are available if knowledge of the solution space is expanded and algorithms that employ the dynamical relationships are developed.

Restricted Problem of Three Bodies

Lissajous trajectories are three dimensional (3-D) quasi-periodic solutions in the 6-D phase space associated with the three-body problem. Under certain conditions, a special subset of Lissajous trajectories emerges – precisely periodic solutions that have been labeled halo orbits. Halo orbits as originally defined in the circular restricted three-body problem, that is, precisely periodic, do not exist in a general ephemeris model with perturbations such as solar radiation pressure and non-periodic primary motion. However, Lissajous trajectories can still be generated and careful selection of in-plane and out-of-plane amplitudes will produce a Lissajous trajectory that is very close to periodic; the label “halo orbits” usually includes such variations. Halo orbits and Lissajous trajectories are not isolated numerical solutions. They are actually members of extensive families (sets of solutions) with similar characteristics. Currently, they are frequently computed, in conjunction with the transfer paths, using straightforward propagation from Earth launch conditions. A more optimal approach may be to initially identify and design a particular halo orbit and/or Lissajous trajectory to closely match the specifications of the mission of interest; then, the best transfer path from Earth or the most useful trajectory arc to/from another point/orbit in this region can be determined. Previous efforts have produced a numerical process that successfully generates a member of a Lissajous family of solutions⁶.

Of all possible Lissajous trajectories, halo orbits have most frequently been considered as nominal libration point orbits for mission planning. From an analytic approximation as a initial estimate^{7,8}, a periodic halo orbit can be produced numerically. An example of a northern (Class I) L_1 halo orbit is presented in Figs. 1-3. Three planar projections of the orbit are shown with the origin in each plot corresponding to the Sun-Earth/Moon barycenter. The three axes in the figure are defined consistent with the rotating frame typically used in the restricted three-body problem. Thus, the x axis is directed from the larger primary (Sun) to the smaller (Earth/Moon

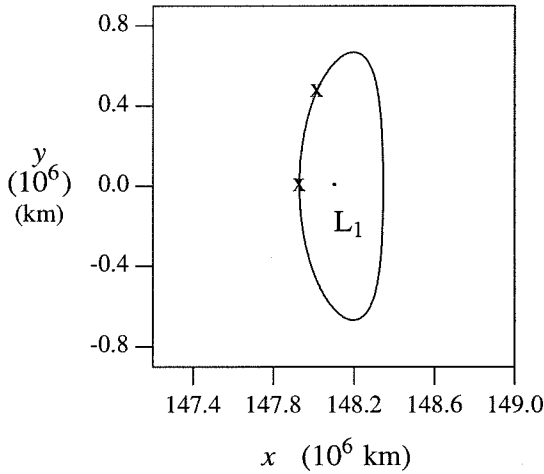


Fig. 1. Halo ($A_z = 120,000$ km): X - Y Projection

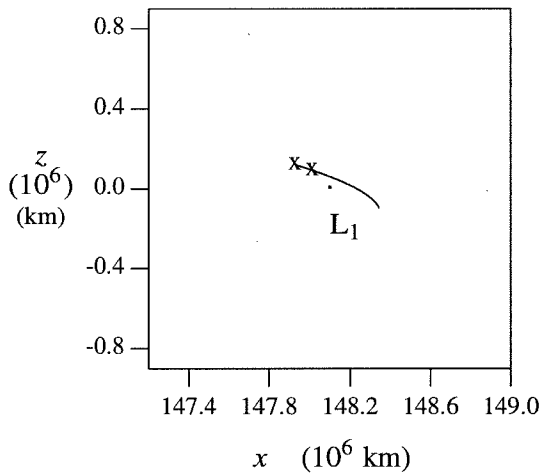


Fig. 2. Halo ($A_z = 120,000$ km): X - Z Projection

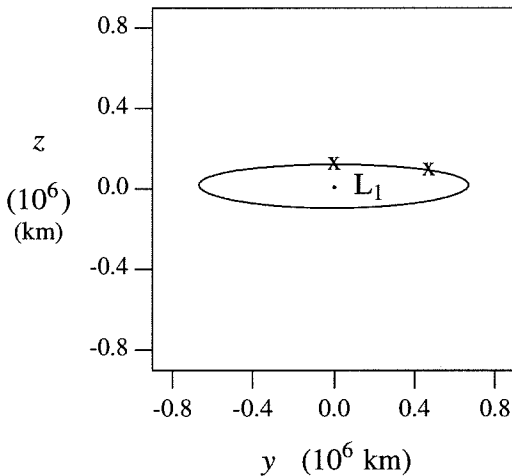


Fig. 3. Halo ($A_z = 120,000$ km): Y - Z Projection

barycenter), the y axis is defined in the plane of motion of the primaries and 90° from the x axis, and the z axis completes the right handed frame. The orbit shown here has an approximate out-of-plane amplitude $A_z = 120,000$ km, which requires the corresponding in-plane amplitudes $A_y = 667,980$ km and $A_x = 208,270$ km. Each revolution has a duration of approximately six months. Note that the spacecraft moves along its path about L_1 in a clockwise direction as viewed in the $y - z$ plane (Fig. 3).

Dynamical Systems and Invariant Manifolds

The geometrical theory of dynamical systems (from Poincaré) is based on the phase portrait of a dynamical system as discussed in various mathematical sources^{9,10}. The geometric model for the set of all possible states of a system is the phase space (or state space), which is assumed to be an open set in \mathbb{R}^n . The state space, filled with trajectories, is the phase portrait of the dynamical system. This portrait may begin with special solutions that include fixed points (or equilibrium points), periodic orbits, quasi-periodic motions, homoclinic and heteroclinic motions. Beyond these solutions, flat Euclidean spaces will not suffice for all geometric models; in some cases, curved spaces (differential manifolds) are necessary. The manifold then becomes the geometrical model for the space of dependent variables.

A manifold is an m -dimensional analog of a two-dimensional surface in \mathbb{R}^n . To provide familiarity and intuition, manifolds will be called m -dimensional surfaces in this discussion. Thus, an invariant manifold is a surface (m -dimensional) defined by the following property: orbits starting on the surface remain on the surface throughout the course of their dynamical evolution. So, an invariant manifold is a collection of orbits that form a surface. Additionally, the set of orbits that approach or depart an invariant manifold asymptotically are also invariant manifolds (under certain conditions) which are called stable and unstable manifolds, respectively. In reaching toward a complete understanding of the global dynamics, knowledge of the invariant manifolds of a dynamical system as well as the interactions of their respective stable and unstable manifolds is absolutely essential.

In the three-body problem, the six-dimensional phase space can be envisioned as composed of subspaces of various dimensions. Thus far, the link to these subspaces, or manifolds, has been the periodic halo orbits and the quasi-periodic Lissajous trajectories in the vicinity of libration points. In the context of the three-body problem, the libration points, halo orbits, and the tori on which Lissajous trajectories

are confined, are themselves invariant manifolds. In this study, the periodic halo orbits are used as the reference solution for investigating the phase space. It is possible to exploit the hyperbolic nature of these libration point orbits by using the associated stable and unstable manifolds to generate transfer trajectories as well as general trajectory arcs in this region of space. The first concern, then, is the computation of the stable and unstable manifolds associated with a particular halo orbit. The procedure is based on the availability of the monodromy matrix associated with the halo orbit. This matrix essentially serves to define a discrete linear map of a fixed point in some arbitrary Poincaré section. As with any discrete mapping of a fixed point, the characteristics of the local geometry of the phase space can be determined from the eigenvalues and eigenvectors of the monodromy matrix. These are characteristic not only of the fixed point, but of the halo orbit itself.

The local approximation of the stable (unstable) manifold involves calculating the eigenvectors of the monodromy matrix that are associated with the stable (unstable) eigenvalues, and then using the state transition matrix to propagate the approximation to any point on the halo. The eigenvalues are known to be of the following form^{4,5}:

$$\lambda_1 > 1, \lambda_2 = (1/\lambda_1) < 1, \lambda_3 = \lambda_4 = 1, \\ \lambda_5 = \lambda_6^*, \text{ and } |\lambda_5| = |\lambda_6| = 1,$$

where λ_5 and λ_6 are complex conjugates. Stable (and unstable) eigenspaces, E^s (E^u) are spanned by the eigenvectors whose eigenvalues have modulus less than one (modulus greater than one). There exist local stable and unstable manifolds, W_{loc}^s and W_{loc}^u , tangent to the eigenspaces at the fixed point and of the same dimension¹⁰. Thus, for a fixed point X^H defined along the halo orbit, the one-dimensional stable (unstable) manifold is approximated by the eigenvector associated with the eigenvalue λ_2 (λ_1). First, consider the stable manifold. Let Y^{W^s} denote a six-dimensional vector that is coincident with the stable eigenvector and is scaled such that the elements corresponding to position in the phase space have been normalized. This vector serves as the local approximation to the stable manifold (W^s). Remove the fixed point X^H from the stable manifold to form two half-manifolds, W^{s+} and W^{s-} . Each half-manifold is itself a manifold consisting of a single trajectory. Now, consider some point X_o on W^{s+} . Integrating both forward and backward in time from X_o produces W^{s+} . Thus, calculating a half-manifold can be broken down into two steps: locating or approximating a point on W^{s+} , and numerically integrating from this point.

To generate the stable manifold, an algorithm has been employed that was developed to find both the stable and unstable manifolds of a second order system¹¹. The algorithm, however, does not possess any inherent limit to the order of the system, and has been used successfully here. Near the fixed point X^H , W^{s+} is determined, to first order, by the stable eigenvector Y^{W^s} . The next step is then to globalize the stable manifold. This can be accomplished by numerically integrating backwards in time. It also requires an initial state that is on W^{s+} but not on the halo orbit. To determine such an initial state, the position of the spacecraft is displaced from the halo in the direction of Y^{W^s} by some distance d such that the new initial state, denoted as $X_o^{W^s}$, is calculated as

$$X_o^{W^s} = X^H + d Y^{W^s}. \quad (1)$$

Higher order expressions for $X_o^{W^s}$ are available but not necessary. The magnitude of the scalar d should be small enough to avoid violating the linear estimate, yet not so small that the time of flight becomes too large due to the asymptotic nature of the stable manifold. This investigation is conducted with a nominal value of 200 km for d . Note that a similar procedure can be used to approximate and generate the unstable manifold.

Visualizing Manifolds

In most texts dealing with dynamical systems theory, lower dimensional problems are usually considered. This setting generally makes it easier to understand the mechanics and to visualize the behavior of the system. When adding the complexity of higher dimensional systems (e.g., six dimensions), conceptual understanding becomes more difficult. In the case of halo orbits in the restricted three-body problem, the stable and unstable manifolds for any fixed point along the halo are one dimensional. This then implies that the stable and unstable manifolds for the *entire* halo orbit are two dimensional. This is an important concept when considering design options. Thus, it would be helpful in understanding the solution space if these 2-D surfaces could be visualized. While it is not possible to graphically represent a two dimensional surface in the full six dimensional phase space, much can still be gained conceptually by projecting this surface onto the three dimensional configuration space.

As an example, consider a halo orbit near L_1 , in the Sun-Earth/Moon system, one with an A_2 amplitude of approximately 150,000 km. A limited set of points is selected in some specified part of the halo; this relatively small region along the path is identified in Figs. 1-3 as all the points in the shorter arc

defined by the “x”s that are seen in each projection. The part of the halo identified in the figures is not selected arbitrarily; rather, it is already known that manifolds computed using these points will pass close to the Earth. For convenience, this region along the halo will be designated the EA (Earth Access) region. Each point in the EA region can be defined as a fixed point X^H and its corresponding one dimensional stable manifold is then globalized. Together, these one dimensional manifolds form the two dimensional manifold associated with this region of the halo orbit. Several views of the projection of this surface onto configuration space are shown in Fig. 4. Beginning with an $x - y$ projection in the upper left, a series of views is presented in the figure. The views are ordered, top to bottom, to represent an observer moving in a positive sense about the x -axis. Thus, the view in Fig. 4c is the $x - z$ projection. The dramatic bend/twist in the surface corresponds to the close passage of the manifold by the Earth (closest approach is approximately 11,000 km). Observe how “narrow” the surface becomes as it approaches the halo versus how “broad” it is between the Earth and the halo. The behavior of this portion of the stable manifold would seem to suggest that targeting some state on the manifold well before it approaches the halo would be easier than targeting a specific point on the halo orbit itself. With the broader surface further away from the halo, more options may become available. Another observation is the “twisting” and “folding” of the manifold near the Earth as seen in Fig. 4. This implies that a variety of options (various combinations of altitudes, inclinations, etc.) may exist for insertion directly onto the manifold near the Earth. It is important to note that the particular characteristics of the manifold that are observed here are not unique to this halo or the stable manifold, i.e., they can be seen on halos of any size for both stable and unstable manifolds alike. Thus, corresponding to unstable manifolds, these observations offer Earth return options as well.

Solutions Using Stable and Unstable Manifolds

Earth-to-Halo Transfers

The design procedure for transfers from the Earth to a halo orbit is frequently based on a shooting method, where a set of initial conditions near Earth is selected, then propagated forward in time; the initial state is adjusted to achieve an acceptable result. This process can be modified, of course, to incorporate backwards integration. The procedure is complicated by the fact that there are no analytic expressions or approximations to provide a guess to initiate the process. Unfortunately, there is also a lack of

control over the final complete solution; the high sensitivity of the resulting halo orbit relative to slight changes in the initial conditions near the Earth make it very difficult to achieve a set of precise characteristics that may be specified for the desired halo or Lissajous orbit.

As an alternative, the stable manifold may offer design options for Earth-to-halo transfers. Conceptually, the transfer design process consists of identifying the subspace (or surface, as seen, for example, in Fig. 4) that contains the endpoints of the boundary value problem - the “endpoints” are, in fact, orbits - and then moving on the surface from the point (orbit) of origin to the destination orbit. So, rather than a targeting problem to reach a specified insertion point on the halo orbit, the transfer design problem becomes one of insertion onto the manifold, directly from the Earth parking orbit, if possible. Using stable/unstable manifolds to construct transfer trajectories from the Earth to the halo orbit implies an asymptotic approach toward the halo, and thus, may result in no halo orbit insertion maneuver. The flight time along such a transfer path is actually very reasonable. The resulting algorithm based on this concept has been very successful at quickly producing insight into the problem as well as generating Earth-to-halo transfer trajectories^{4,5}. A distinct advantage of this approach is that the designer ultimately has more control over each aspect of the trajectory; and, the transfer path emerges *without* a random search process. Unfortunately, not every halo orbit possesses stable manifolds that pass at the precise altitude of the specified Earth parking orbit. In particular, as the size of the halo orbit decreases, the associated stable manifolds move further away from the Earth until direct insertion onto a manifold from the parking orbit is no longer possible for a direct transfer. This corresponds to the well known observation that more ΔV is required to insert into a small halo/Lissajous orbit. The stable/unstable manifolds control the behavior of all nearby solutions in this region of the phase space. Thus, the behavior of the manifolds can provide insight into optimal insertion locations along the halo, and the manifolds may serve as a first guess for use in a differential corrections scheme⁴. The application of this approach can be seen in Figs. 5 and 6, where a transfer trajectory is presented as viewed in a rotating coordinate frame. The plot represents the $x - y$ (Fig. 5) and the $x - z$ (Fig. 6) projections of a transfer to the halo orbit near L_1 shown in Figs. 1-3 (roughly the same size as the halo used for ISEE-3). The halo orbit is denoted by dots. With an A_z amplitude of 120,000 km, this halo is too small for its stable manifolds to pass the Earth at a reasonable parking

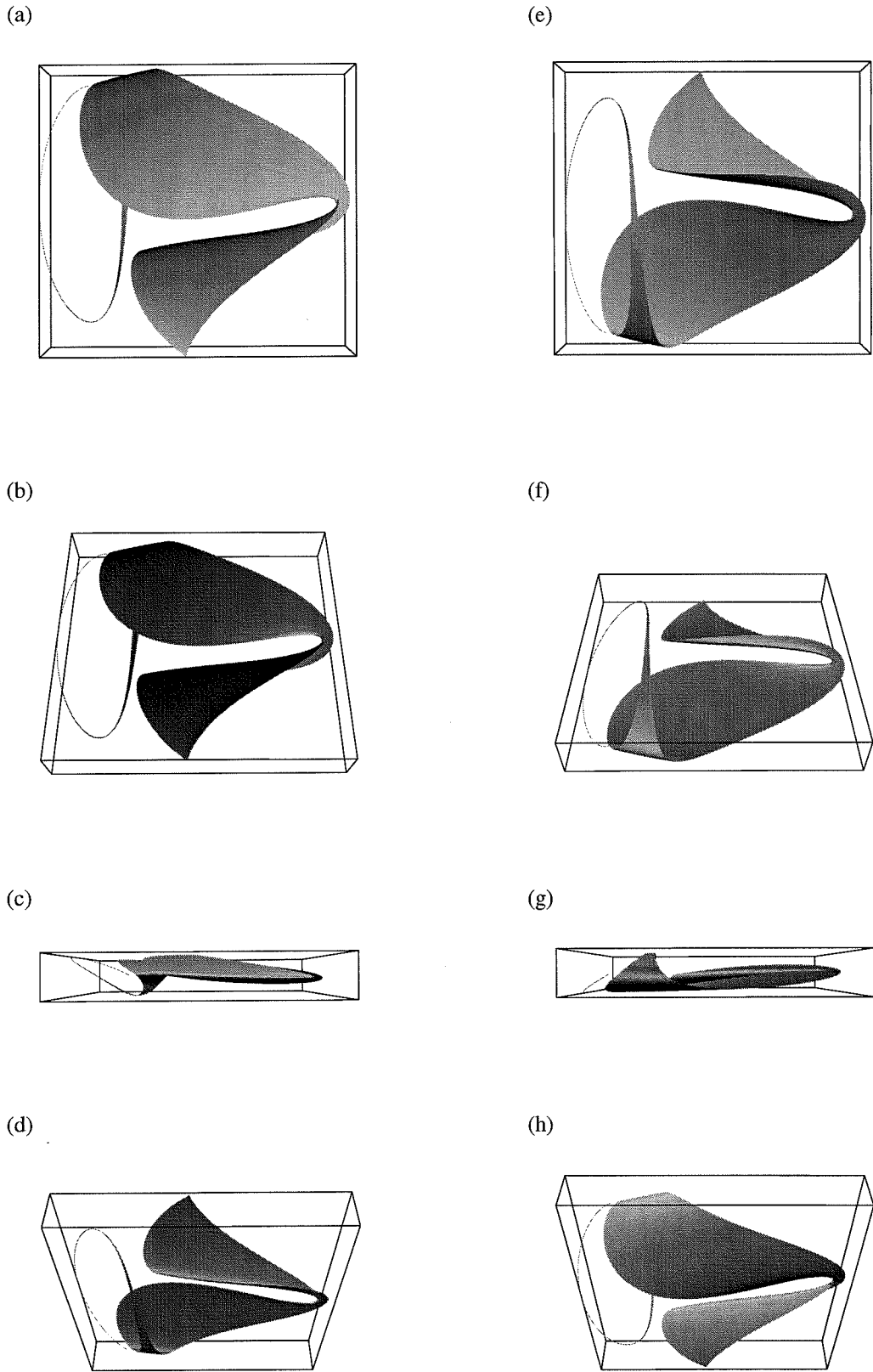


Fig. 4. Projection of a Portion of the Stable Manifold onto Configuration Space

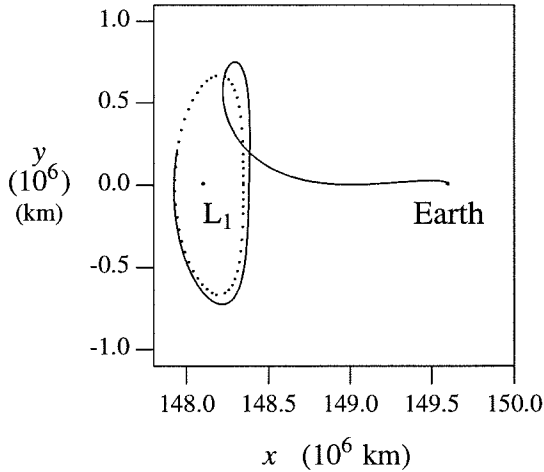


Fig. 5. Earth-to-Halo Transfer; Insertion Cost = 20.8 m/s; X - Y Projection

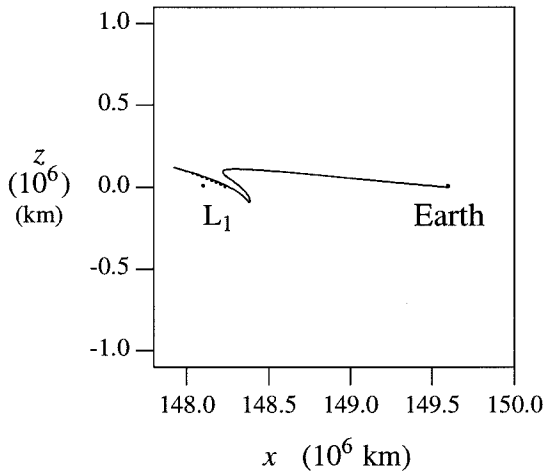


Fig. 6. Earth-to-Halo Transfer; Insertion Cost = 20.8 m/s; X - Z Projection

orbit altitude (for a direct transfer), i.e., no “free” direct transfers exist. It is therefore necessary to introduce a maneuver. By understanding the behavior of the stable manifolds, a point along the halo can be identified that is associated with a manifold that passes closest to the Earth; note that the best choice is a point in the EA region that is identified in Figs. 1-3. The trajectory approaches the halo orbit along a natural pathway that results in a lower cost. In this case, the maneuver is placed at the halo orbit insertion point and has a value of 20.8 meters/second. Time and effort to produce results of this type are minimal and the process can be automated^{4,5}.

Halo-to-Earth Transfers

As mentioned previously, similar consideration can

be given to the use of the unstable manifold when exploring trajectory options. One possible application involves a return trajectory, i.e., a transfer from a halo orbit to the Earth. As a demonstration of this option, consider a halo orbit near L_2 that is much larger than the one considered previously ($A_2 = 569,275$ km). This particular libration point orbit is shown in Figs. 7 and 8. A point along the path is identified for computation of the unstable manifold; this point also belongs to the EA region in this (Class II) southern L_2 orbit. In contrast to the relatively small halo used in Figs. 5 and 6, the manifolds corresponding to this large L_2 halo pass arbitrarily close to the Earth. Proceeding as before, a study of the behavior of solutions on the unstable manifold indicates the existence of a solution that asymptotically departs the halo orbit and results in a close approach of the Earth at an altitude of 185 km (this number can be made smaller or larger).

Halo-to-Halo Transfers

The concepts underlying the Earth-to-halo and halo-to-Earth transfers can be combined to investigate new families of solutions in the three-body problem. By proper choice of the parameter d in Eqn. (1), both stable and unstable manifolds can be used to produce transfers between halo orbits and Lissajous trajectories^{4,5}. A search for halo-to-halo transfers yields various options. Consider two halo orbits that are close in size; one is near L_1 , the other is near L_2 , and both can be pre-determined. For now, the L_1 halo is designated as the departure orbit. A point along the L_1 halo is selected as the departure point. This choice is based on observations of the behavior of the manifolds in different regions along the halo, i.e., the point whose unstable manifold approaches an L_2 Lissajous upon globalization. Then, in similar fashion, a stable manifold associated with an L_2 halo orbit is computed that approaches an L_1 Lissajous upon backwards integration. Once both manifolds have been generated, the locations that represent the minimum distance between the manifolds is determined, and these are defined as the end states of each. Almost certainly, there will be a discontinuity between these two states. Since the goal is a solution that is continuous in position, a differential corrections scheme is introduced to drive the end states of both the forward and backward paths to some mutual target point (in position) between them by introducing ΔV 's at the “initial” points near the halos. The final result is a transfer with three maneuvers (typically): one at each halo orbit and one at the patch point (the mutual target point between the end states).

The first example of this procedure is shown in

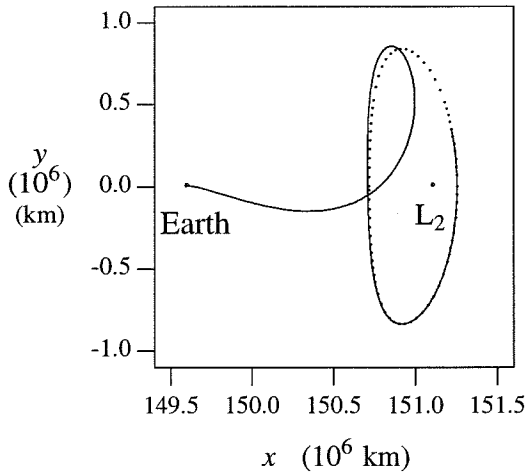


Fig. 7. Halo-to-Earth Transfer; No Departure Cost: X - Y Projection

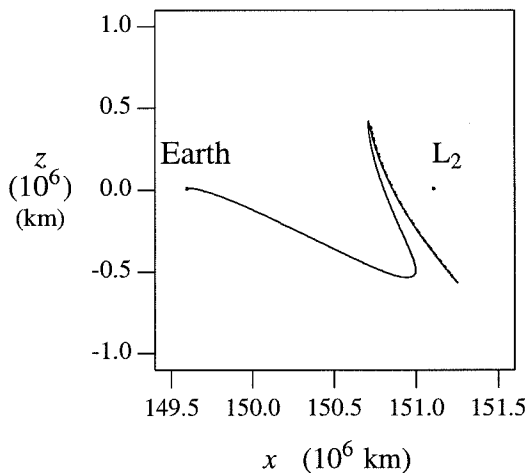


Fig. 8. Halo-to-Earth Transfer; No Departure Cost: X - Z Projection

Figs. 9 and 10. Here, the L_1 halo is designated as the departure halo and L_2 as the arrival halo. Both are northern (Class I) halo orbits with out-of-plane amplitudes of approximately 492,000 km and 483,000 km, respectively. The total ΔV for the transfer is 40.63 m/s; the ΔV s near the halos are 0.86 m/s and 3.60 m/s, respectively, and a 36.17 m/s velocity discontinuity exists at the patch point (marked with an "o"). This procedure has been applied to halos of various sizes and the costs have been similar⁵.

Another example of the application of this same procedure to determine different types of solutions is shown in Figs. 11 and 12. In this case, the L_1 halo is a northern (Class I) halo with an out-of-plane amplitude of approximately 537,000 km, and the L_2 halo

is a southern (Class II) halo with an A_z of approximately 554,000 km. The final trajectory has maneuvers of 6.76 m/s at the L_1 halo departure point, 42.01 m/s at the patch point (marked with an "o" in Figs. 11 and 12), and no maneuver at the L_2 halo arrival for a total cost of 48.77 m/s. Numerical evidence suggests that this type of trajectory does not exist for halos that are smaller than those presented here. It is important to note that none of the examples discussed here have been optimized.

Suess-Urey Trajectory Design

Mission Goals and Constraints

Planetary scientists have recently expanded their efforts to exploit the scientific potential of libration point trajectories. Thus, more proposals now use Lissajous trajectories as a centerpiece of the mission design. One such example is the recently proposed Suess-Urey (SU) mission. The primary goal of SU is to collect solar wind particles for a period of approximately two years, and then analyze their chemical and isotopic compositions. Solar wind particles do not strike the Earth due to the Earth's magnetic field. Collection of these particles must then be carried out beyond the influence of the Earth's magnetic field making a Lissajous orbit near L_1 an ideal platform. The analysis of the solar wind contents is to be accomplished on Earth which mandates an Earth return trajectory from the L_1 Lissajous. Upon return, a capsule will reenter the atmosphere to be captured by a helicopter in mid-air after deceleration; the need for a day side reentry is apparent. The geographical target is the Utah Test and Training Range (UTTR), with the additional constraint of a west-east approach. These mission goals can now be summarized with the following preliminary design constraints: 1) transfer from a low Earth parking orbit to a Lissajous trajectory near L_1 ; 2) maintain the Lissajous orbit for two years (four revolutions); 3) return for a day side reentry into the Earth's atmosphere with a declination of 40.6° (location of UTTR) and an inclination as low as possible (due to west-east approach). These constraints combine to form a very complex mission that serves as an excellent opportunity to demonstrate the construction of a continuous trajectory from trajectory arcs (on the manifolds) in the three-body problem.

Preliminary Study in the Restricted Problem

This investigation begins in the circular restricted problem using the Sun as the larger primary and the Earth/Moon barycenter (mass equal to the sum of the masses of the Earth and Moon) as the second primary, consistent with the previous discussion. The

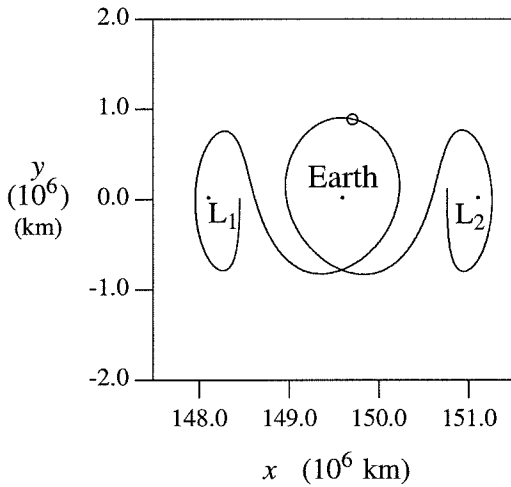


Fig. 9. Halo-to-Halo Transfer; 40.63 m/s: $X - Y$ Projection

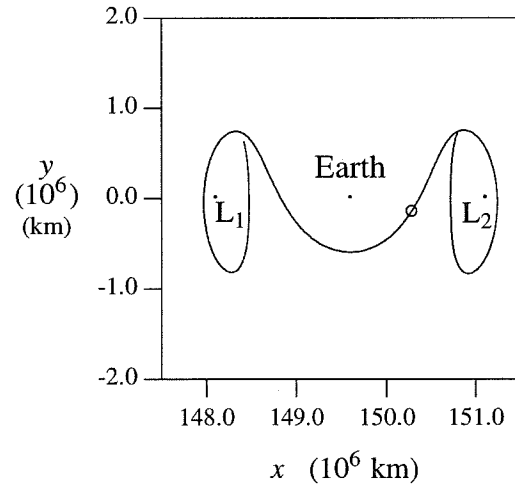


Fig. 11. Halo-to-Halo Transfer; 48.77 m/s: $X - Y$ Projection

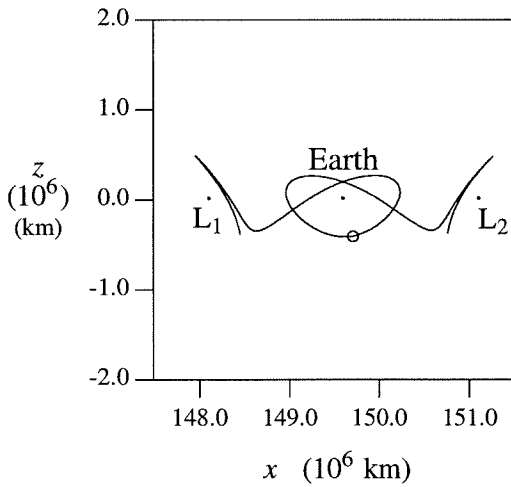


Fig. 10. Halo-to-Halo Transfer; 40.63 m/s: $X - Z$ Projection

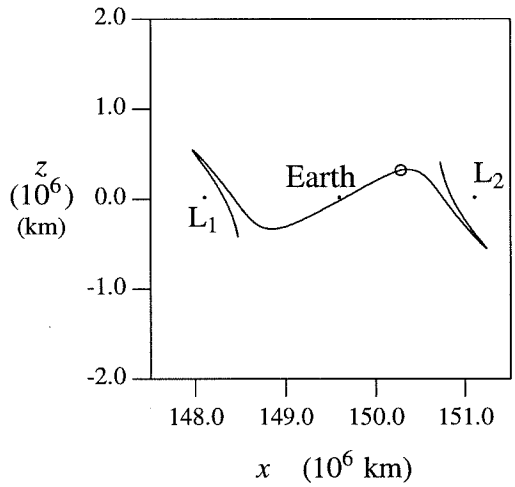


Fig. 12. Halo-to-Halo Transfer; 48.77 m/s: $X - Z$ Projection

objective in using this model is to establish the qualitative nature of solutions that may satisfy the mission constraints. However, the results from a study in the restricted problem will translate very well into the more complicated model that incorporates ephemeris data. Use of this model also allows straightforward application of dynamical systems theory.

Using the concepts discussed in connection with Figs. 5 and 6, Figs. 7 and 8, and Figs. 11 and 12, the general shape of the transfer out from Earth, the L_1 Lissajous, and the Earth return begins to emerge. The mission constraint that has the most impact on the shape of the trajectory is the day side reentry requirement. Recall from the definition of the rotating coordinate system that the Sun is in the negative x

direction at all times. The ΔV that would be needed for a direct return from the L_1 Lissajous with a day side reentry would be prohibitive. A return from a Lissajous near L_2 , however, would allow a direct day side return. Figures 7 and 8 illustrate the potential use of the unstable manifold associated with a halo near L_2 to accomplish this task. To be a legitimate option, a transfer from the L_1 halo to the L_2 halo must be realized. Figs. 11 and 12 exhibit one option for such a transfer.

Before proceeding with trajectory construction, however, further investigation of the unstable L_1 manifold is helpful. In particular, arcs (on the manifold) are sought that leave the L_1 halo and approach the Earth in a manner consistent with a combination

of the trajectory segments in Figs. 11 and 12 and Figs. 7 and 8. Consider then, a halo orbit near L_1 with an A_z amplitude of approximately 518,000 km. A short investigation of the manifolds originating from different regions of the halo quickly provides a clearer view of the type of trajectory that will satisfy the mission requirements. The $x - y$ and $x - z$ projections of one of the unstable manifolds are seen in Figs. 13 and 14. Thus, an Earth Access region for halo departure has been established, one that results in the desired day side reentry. A two dimensional surface can be computed that is associated with this EA region. A closer look at the surface of unstable manifolds will provide useful information regarding the inclination and declination issues.

A number of views of the projection of the surface onto configuration space (similar to Fig. 4) are seen in Fig. 15. Contrary to Fig. 4, only the region near the Earth is presented in Fig. 15. The important observation here is the two basic types of Earth approach. Some manifolds approach the Earth with very high inclinations relative to the ecliptic (as high as 74.2°); then there is a transition to a region where the manifolds approach with much lower inclinations (as low as 50.7°). This will clearly impact the west-east reentry requirement.

The size of the L_1 halo orbit used to generate Figs. 13 through 15 is not an arbitrary choice. An orbit of this size is necessary to approach the L_2 region in the manner that would meet the mission requirements (recall that halo-to-halo transfers of this type do not exist for smaller halos). It was also selected because none of the unstable manifolds originating from the designated EA region of the halo pass closer than 125 km altitude above the Earth. However, it is more desirable for the mission to use a smaller halo/Lissajous near L_1 , and eventually, it will be necessary to employ an unstable manifold that reaches closer to L_2 (which would require a even larger halo orbit near L_1). It now becomes necessary and appropriate to patch trajectory arcs together. As an example, consider a smaller halo ($A_z = 450,000$ km) near L_1 and a larger halo ($A_z = 565,000$ km) also near L_1 . A similar study of the unstable manifolds is done on both halos. In the case of the *larger* halo, a 1-D unstable manifold is computed such that the approach to the Earth is in the region of lower inclinations (as opposed to the higher inclinations seen in Fig. 15), and passes at a reasonable altitude as well. Then, for the *smaller* halo, a 1-D manifold is determined with the same $x - z$ plane crossing (after leaving the vicinity of the halo) as the larger halo. This crossing point will serve as one of the patch points. Now, another point is chosen on the manifold corresponding to the

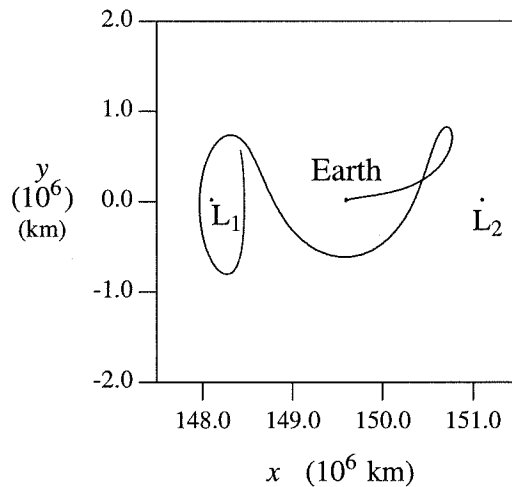


Fig. 13. Unstable Manifold for Halo with $A_z = 565,000$ km

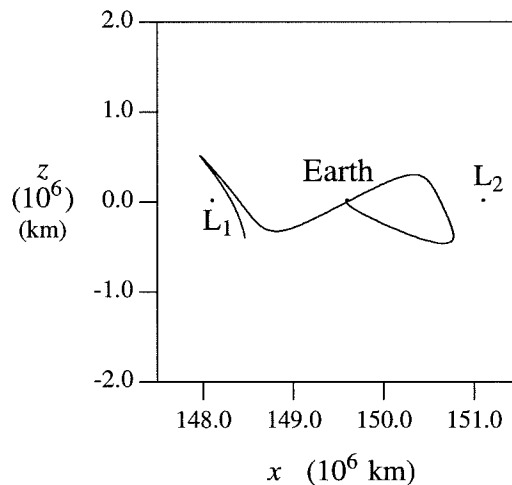


Fig. 14. Unstable Manifold for Halo with $A_z = 565,000$ km

larger halo near L_2 . The same differential corrections technique used to generate the halo-to-halo transfers is then applied here. Finally, the trajectory is completed by adding the initial segment, i.e., the transfer out from the Earth to the L_1 halo. Using the stable manifold (as with Figs. 5 and 6), a “free” transfer can be generated from a parking orbit of 185 km (arbitrary). The final two segments that comprise the return are presented in Figs. 16 and 17. Each patch point is marked with an “o.” While there is no maneuver for the halo orbit insertion, some ΔV is required at the other patch points. At this stage, however, the more important information is the qualitative characteristics and using them to guide the design process in the full model.

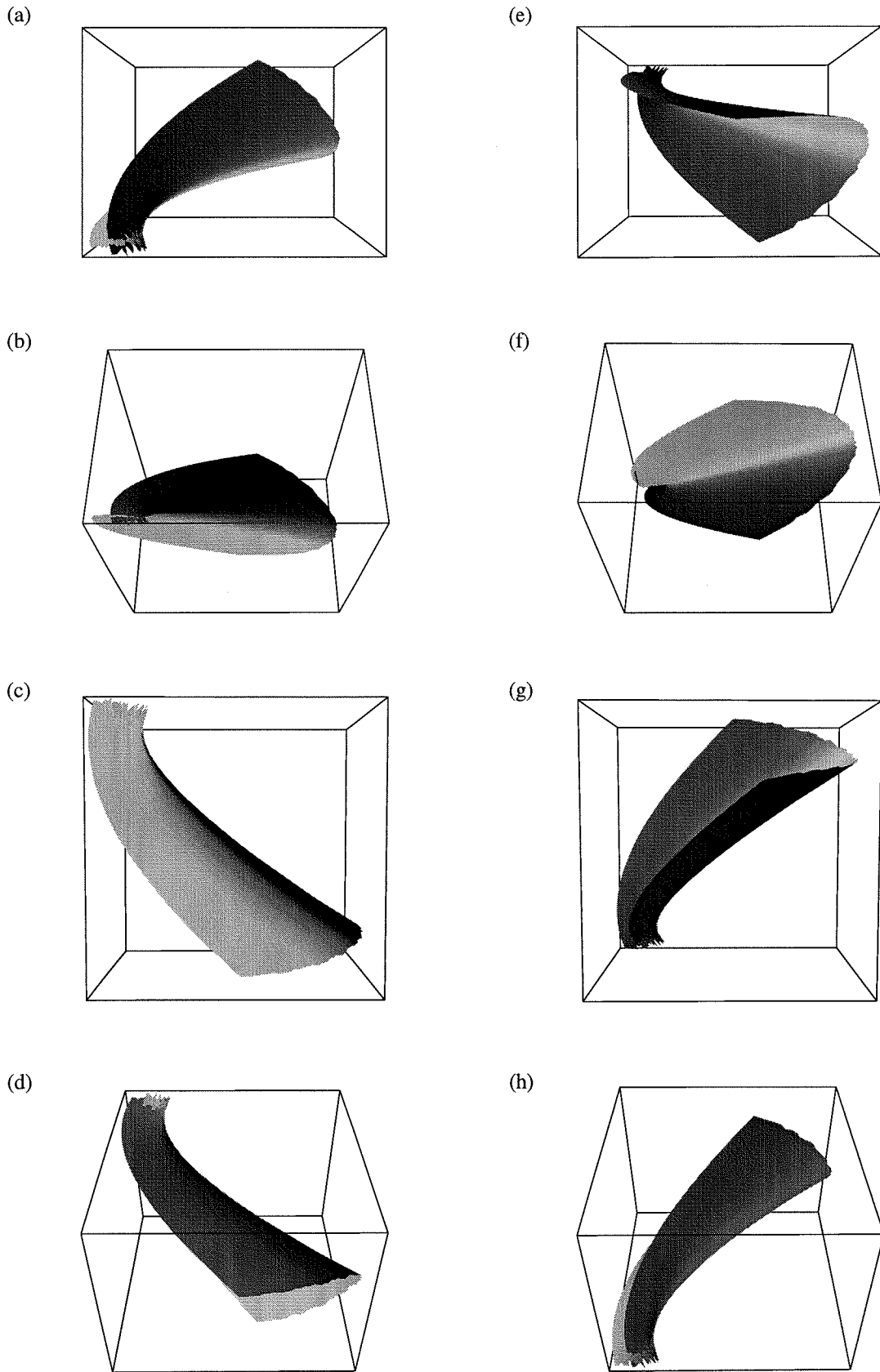


Fig. 15. Unstable Manifold Near Earth

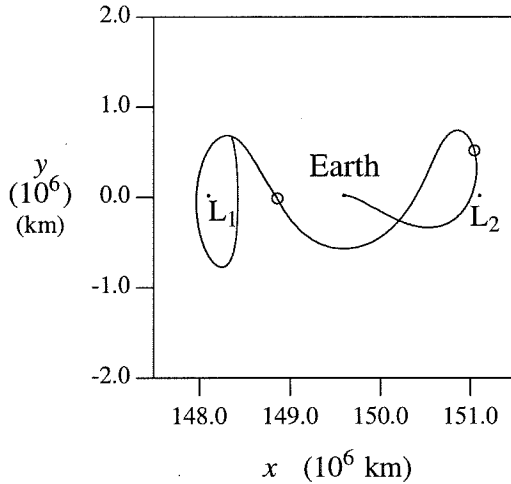


Fig. 16. Patched Solution in Restricted Problem

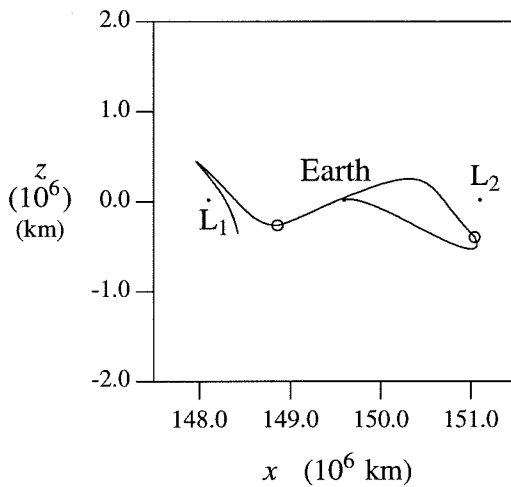


Fig. 17. Patched Solution in Restricted Problem

Solution in Model Using Ephemerides

The qualitative characteristics of the trajectory in Figs. 16 and 17 will now serve as a guide for the final and complete result in the full model that includes ephemerides and solar radiation pressure. It is now appropriate to list more specific mission requirements for the trajectory: 1) transfer directly to an L_1 Lissajous from an Earth parking orbit with an altitude of 200 km and an inclination (relative to the equator) between 28.5° and 31.0° ; 2) maintain the spacecraft in the vicinity of L_1 for two years; 3) return to Earth with a nominal altitude of 200 km at perigee on the day side; 4) two days before perigee, perform a maneuver that will result in an altitude of 125 km with a flight path angle of -7.9° , declination of 40.6° , a longitude of -114.6° , and a west-east approach.

One possibility that satisfies each of the mission re-

quirements is presented in Figs. 18 ($x-y$ projection) and 19 ($x-z$ projection). These figures are plotted in the rotating/oscillating libration point frame with the origin at L_1 . Each significant maneuver is marked with an "o." The trajectory begins in a circular parking orbit with an altitude of 200 km and an inclination of 29.0° . The direct transfer to the Lissajous orbit is initiated with an impulsive tangential ΔV of approximately 3.2 km/s. Approximately 195 days later (at the far $x-z$ plane crossing), the spacecraft executes the Lissajous orbit insertion maneuver (LOI) into a Lissajous trajectory with approximate amplitudes of $A_z = 320,000$ km, $A_x = 220,000$ km, and $A_y = 700,000$ km. Over the next four revolutions around the Lissajous, small maneuvers (less than 1 m/s) may be executed to maintain the orbit as well as initiate the return portion of the trajectory. A little more than two years after LOI, as the spacecraft departs the vicinity of L_1 , a maneuver of 36.6 m/s is performed at the $x-z$ crossing approximately midway between L_1 and the Earth. This propels the spacecraft on the transfer from L_1 to the vicinity of L_2 . En route to L_2 , the spacecraft passes near the Lunar orbit, but there is no Lunar encounter. As the spacecraft approaches L_2 , another maneuver of 14.3 m/s is implemented to set up the return. This time, as the spacecraft crosses the Lunar orbit, there is a distant lunar encounter. Shortly after this encounter, a final ΔV of 3.5 m/s is executed to lower perigee and initiate reentry at an altitude of 125 km with a declination of 40.6° , a longitude of -114.6° , an inclination of 49.7° , and a flight path angle of -7.9° . Final reentry is scheduled to be on September 18, 2002. Table 1 provides a summary of the major trajectory events.

Conclusions

The similarities between Figs. 18 and 19 and Figs. 16 and 17 provide much encouragement for use of the restricted problem to capture the qualitative characteristics of the design space. With the use of dy-

Table 1. Suess-Urey Trajectory Summary

Event	Date (m/d/y)	Altitude (km)	ΔV (m/s)
Earth Launch	08/22/99	200	3193.6
LOI	03/04/00		11.4
Maneuver	04/25/02		36.6
Maneuver	07/06/02		14.3
Lunar Encounter	09/16/02	100,000	
Maneuver	09/16/02		3.5
Reentry	09/18/02	125	

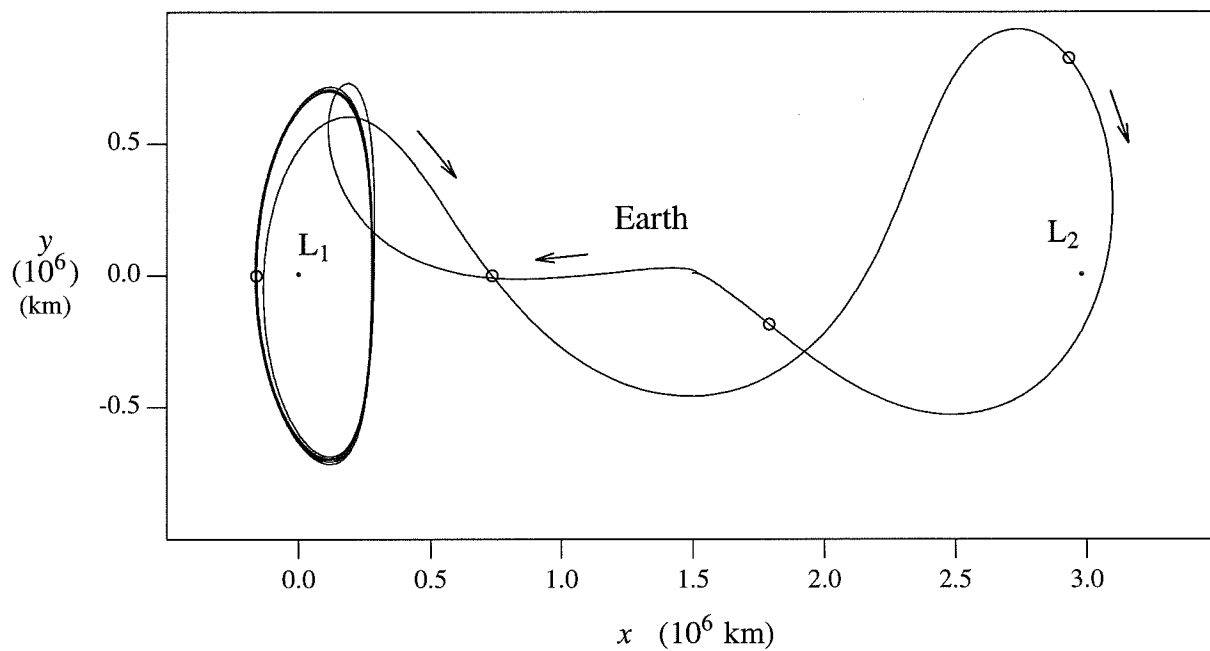


Fig. 18. One Option for Sues-Urey Mission: X - Y Projection

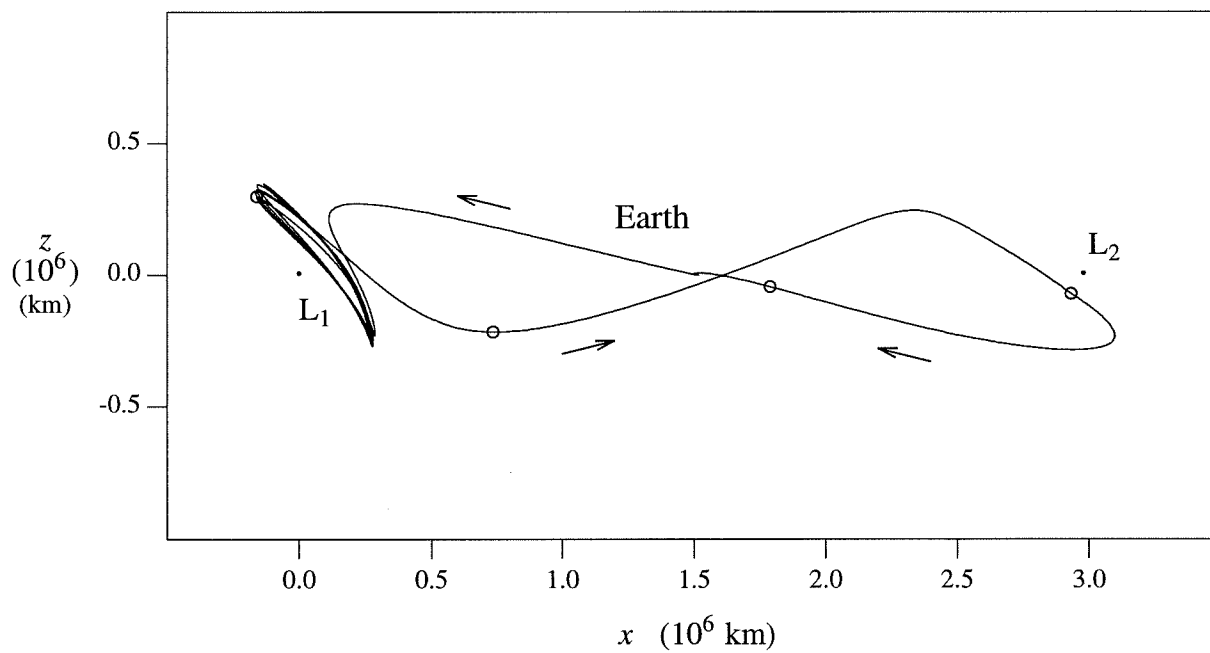


Fig. 19. One Option for Sues-Urey Mission: X - Z Projection

namical systems theory, investigating trajectory options in the restricted problem becomes much more efficient. It also provides important insight into the natural dynamics of this highly complex system: not only are the natural solutions exposed, but potential problems can also be identified (as was demonstrated in Fig. 15 with the high and low inclination reentries). While the advantage of using dynamical systems theory in the restricted problem is clear, application to the more complex model is still under development.

Acknowledgments

The authors would like to thank Eric Campbell of Purdue University for his input on the no-revolution halo-to-halo transfer. Portions of this work were carried out at the Jet Propulsion Laboratory, California Institute of Technology, and at Purdue University, under a contract with the National Aeronautics and Space Administration.

References

- ¹G. Gómez, A. Jorba, J. Masdemont, and C. Simó, "Final Report: Study Refinement of Semi-Analytical Halo Orbit Theory," ESOC Contract Report, Technical Report, April 1991.
- ²G. Gómez, A. Jorba, J. Masdemont, and C. Simó, "Study of the Transfer from the Earth to a Halo Orbit Around the Equilibrium Point l_1 ," Technical Report, December 1991.
- ³G. Gómez, A. Jorba, J. Masdemont, and C. Simó, "Moon's Influence on the Transfer from the Earth to a Halo Orbit Around l_1 ," Technical Report.
- ⁴K. C. Howell, D. L. Mains, and B. T. Barden, "Transfer Trajectories from Earth Parking Orbits to Sun-Earth Halo Orbits," *Cocoa Beach, Florida*, Vol. 41, February 14-16 1994.
- ⁵B. T. Barden, "Using Stable Manifolds to Generate Transfers in the Circular Restricted Problem of Three Bodies," M.S. Thesis, School of Aeronautics and Astronautics, Purdue University, West Lafayette, Indiana, December 1994.
- ⁶K. C. Howell and H. J. Pernicka, "Numerical Determination of Lissajous Trajectories in the Restricted Three-body Problem," *Celestial Mechanics*, Vol. 41, 1988, pp. 107-124.
- ⁷C. Marchal, "Study on the Analytic Representation of Halo Orbits," ESA Contractor Final Report, Contract Report No. 5647/83/D/JS(SC), Technical Report, July 1985.

⁸D. L. Richardson, "Analytic Construction of Periodic Orbits About the Collinear Points," *Celestial Mechanics*, Vol. 22, 1980, pp. 241-253.

⁹S. Wiggins, *Introduction to Applied Nonlinear Dynamical Systems and Chaos*. New York: Springer-Verlag, 1990.

¹⁰J. Guckenheimer and P. Holmes, *Nonlinear Oscillations, Dynamical Systems, and Bifurcations of Vector Fields*. New York: Springer-Verlag, 1983.

¹¹T. S. Parker and L. O. Chua, *Practical Numerical Algorithms for Chaotic Systems*. New York: Springer-Verlag, 1989.